

1 **Stable Engraftment of a Human Gut Bacterial Microbiome in Double Humanized BLT-mice**

2 Lance Daharsh^{1,2}, Amanda E. Ramer-Tait³, *Qingsheng Li^{1,2}

3

4 ¹Nebraska Center for Virology, ²School of Biological Sciences, ³Department of Food Science and
5 Technology, University of Nebraska-Lincoln, Lincoln, NE 68583, USA

6

7 Corresponding author: Qingsheng Li (qli@unl.edu)

8

9 **Abstract**

10 **Background**

11 Humanized mice featuring a functional human immune system are an important pre-clinical
12 model for examining immune responses to human-specific pathogens. This model has been
13 widely utilized to study human diseases that are otherwise impossible or difficult to investigate
14 in humans or with other animal models. However, one limitation of using humanized mice is
15 their native murine gut microbiome, which significantly differs from the one found in humans.
16 These differences may be even greater for mice housed and bred in specific pathogen free
17 conditions. Given the importance of the gut microbiome to human health and disease, these
18 differences may profoundly impact the ability to translate the results from humanized mice
19 studies to human disease. Further, there is a critical need for improved pre-clinical models to
20 study the complex *in vivo* relationships of the gut microbiome, immune system, and human
21 disease. We therefore created double humanized mice with both a functional human immune
22 system and stable human-like gut microbiome.

23 **Results**

24 Surgery was performed on NOD.*Cg-Prkdc^{scid}Il2rg^{tm1Wjl}/SzJ* (NSG) mice to create bone-marrow,
25 liver, thymus (BLT) humanized mice. After immune reconstitution, mice were treated with
26 broad spectrum antibiotics to deplete murine gut bacteria and then transplanted with fecal
27 material from healthy human donors. Characterization of 173 fecal samples obtained from 45
28 humanized mice revealed that double humanized mice had unique 16S rRNA gene profiles
29 consistent with those of the individual human donor samples. Importantly, transplanted
30 human-like gut microbiomes were stable in mice for the duration of the study, up to 14.5 weeks
31 post-transplant. Microbiomes of double humanized mice also harbored predicted functional
32 capacities that more closely resembled those of the human donors compared to humanized
33 mice.

34 **Conclusions**

35 Here, we describe successful engraftment of a stable human microbiome in BLT humanized
36 mice to further improve this preclinical humanized mouse model. These double humanized
37 mice represent a unique and tractable new model to study the complex relationships between
38 the human gut microbiome, human immune system, and human disease *in vivo*.

39

40 **Background**

41 The complex ecosystem of the gut microbiome plays a critical role in human health and
42 disease [1-5]. Specifically, the gut microbiome has a highly reciprocal and dynamic relationship
43 with the immune system. Antigens derived from the gut microbiome influence host immune
44 responses, and the immune system in turn contributes to shaping the spatial distribution and

45 composition of the gut microbiota [6-8]. Humanized mice (hu-mice) with an engrafted human
46 immune system have facilitated important advancements in the study of human cancer,
47 autoimmune diseases, hematopoiesis, and infectious diseases [9-17]. However, gut
48 microbiomes of hu-mice are murine in origin and are often not well-characterized in
49 translational studies. The murine gut microbiome differs substantially in composition and
50 function from that of humans [18], primarily due to anatomical differences as well as other
51 factors such as diet [19]. Considering the importance of the gut microbiota to proper
52 immunological development and influencing immune responses, the murine origin of the
53 microbiome harbored by hu-mice could affect translational study outcomes. Consequently, a
54 need exists to not only characterize the gut microbiomes of hu-mice, but also impart these mice
55 with a more human-like gut microbiome to improve the translational aspects of the model for
56 human medicine.

57 The creation of a new pre-clinical hu-mice model to study the human immune in the
58 context of a human microbiome offers numerous benefits over existing options. Many aspects
59 of human disease are difficult or impossible to study directly in humans due to practical or
60 ethical concerns. Non-human primate models are informative but are genetically outbred, and
61 large studies are often resource and cost prohibitive. Many important discoveries in the
62 microbiome field have been made using mouse models; however, translating results from
63 mouse studies to humans has often proved difficult. The use of germ-free mice reconstituted
64 with human-like gut microbiomes has been the gold standard in studying the relationship of the
65 gut microbiome to human health and disease [20, 21]. However, working with or deriving germ-
66 free animals requires expertise and facilities that are not always available. Further, many

67 immunodeficient mouse strains commonly used to reconstitute a human immune system, such
68 as NOD.*Cg-Prkdc^{scid}Il2rg^{tm1Wjl}/SzJ* (NSG), are currently not commercially available as germ-free.
69 We therefore created a double hu-mice model featuring both a functional human immune
70 system and a stable human-like gut microbiome under specific pathogen free (SPF) conditions.
71 Here, we show that double hu-mice had unique 16S rRNA gene profiles based on the individual
72 human donor sample with which they were colonized. Importantly, the transplanted human-
73 like microbiome was stable in the mice for the duration of the study, up to 14.5 weeks post-
74 transplant. Double hu-mice also harbored gut microbiomes with a more human-like predicted
75 functional capacity compared to their hu-mice counterparts.

76

77 **Results**

78 **Gut microbiomes of double hu-mice are distinct and more human-like compared to hu-mice.**

79 To create double hu-mice, surgery was performed on NSG mice to create bone-marrow,
80 liver, thymus (BLT) hu-mice. Hu-mice were then pre-treated with a cocktail of broad-spectrum
81 antibiotics and administered fecal transplants using fecal material from healthy human donors
82 (see Methods and Daharsh et al.[22] for detailed descriptions and demonstrations). Multiple
83 cohorts of double hu-mice were created using fecal material from one of three unique healthy
84 human donors or an equal mixture of all three (Table 1). We used 16S rRNA gene sequencing
85 and characterized the gut bacterial microbiome of 100 fecal samples from 16 double hu-mice
86 and compared them with 67 fecal samples representing the pre-existing murine gut bacterial
87 microbiomes of hu-mice and the profiles of the 4 human fecal donor samples. To visualize beta-
88 diversity relationships between hu-mice, double hu-mice, and the human donor samples, non-

89 metric multidimensional scaling (NMDS) and principal coordinate analysis (PCoA) plots were
 90 created (Fig. 1). Using NMDS, the gut microbiome profiles of the three groups separated into
 91 distinct clusters (Fig. 1a). Using PCoA, the human donor samples fell within the double hu-mice
 92 hull, which was distinct from the hu-mice profiles (Fig. 1b). Both dimensionality reduction
 93 methods showed that after engraftment of a human gut microbiome, double hu-mice
 94 represented a distinct population that clustered closer to the human donor samples compared
 95 to hu-mice harboring murine gut microbiomes. Importantly, there was no reversion to hu-mice
 96 profiles post-transplant. Displaying the relatedness of the samples through a hierarchical
 97 dendrogram based on Bray-Curtis distances further confirmed the similarity of double hu-mice
 98 microbiomes to the human donor samples and differentiated them from those of hu-mice (Fig.
 99 2).

100 **Table 1. Experimental summary of double hu-mice cohorts**

| Cohort | Antibiotic start | Antibiotic duration | Number of fecal transplants | Human fecal donor | Maximum weeks post-transplant | Double hu-mice | Double hu-mice fecal samples | Hu-mice | Hu-mice fecal samples |
|-------------------|-----------------------------|---------------------|---------------------------------|-------------------|-------------------------------|----------------|------------------------------|---------|-----------------------|
| Antibiotic Pilot | After immune reconstitution | 9 days | 0 | NA | 0 | 0 | 0 | 6 | 9 |
| Donor 65 Cohort 1 | After immune reconstitution | 14 days | 2 (24 & 48 hr post antibiotics) | 65 | 13.5 | 3 | 35# | 3 | 23 |
| Donor 65 Cohort 2 | After immune reconstitution | 14 days | 2 (24 & 48 hr post antibiotics) | 65 | 14.5 | 2 | 16# | 8 | 8 |
| Donor 74 | After immune reconstitution | 7 days | 2 (24 & 48 hr post antibiotics) | 74 | 6 | 3 | 17# | 3* | 3* |

| | | | | | | | | | |
|---|------------------------------|---------|---------------------------------|-------------------------------|---|---|-----|----|----|
| Donor 82 | After immune reconstitution | 7 days | 2 (24 & 48 hr post antibiotics) | 82 | 6 | 4 | 27# | 3* | 3* |
| Donor Mix | 3 days after hu-mice surgery | 14 days | 2 (24 & 48 hr post antibiotics) | Equal mixture of 65, 72, & 84 | 9 | 4 | 21# | 9 | 10 |
| # Includes 1 pre-fecal transplant sample for each of the double hu-mice | | | | | | | | | |
| * Control hu-mice were the same for Donor 74 and Donor 82 groups | | | | | | | | | |

101

102 We also observed that double hu-mice maintained the pre-existing relationships
103 between gut microbiome profiles of the human fecal donors (Fig. 1c & 1d). Importantly, pre-
104 treatment samples from corresponding double hu-mice in each cohort had similar gut
105 microbiome profiles as untreated control hu-mice. After engraftment, double hu-mice
106 resembled the individual human donor that was transplanted as demonstrated by the
107 relationships between the human donor microbiome profiles. Human donors 72 and 84 had
108 more similar profiles to one another than to human donor 65. This relationship was maintained
109 in the double hu-mice after engraftment. We also prepared an “un-biased” human sample by
110 mixing equal parts of the three human donor fecal samples, designated hereafter as donor mix.
111 The microbiome profile of this mixed sample resembled a mixture of the three individual
112 human donor profiles. Specifically, the mixed donor sample more closely resembled individual
113 donors 72 and 84, and this observation was mirrored in the double hu-mice engrafted with the
114 donor mix sample.

115 We also investigated the impact of antibiotic treatment duration on the engraftment of
116 human gut microbiome. The double hu-mice engrafted with human donors 74 and 82 were
117 generated after only 7 days of antibiotic pre-treatment. Their microbiome profiles were less
118 similar to the human donor profiles than those from cohorts pre-treated with antibiotics for 14

119 days prior to fecal transplant (Fig. 1c & 1d). We found the 2 weeks of antibiotic treatment was
120 optimal for the creation of double hu-mice. Together, these results demonstrate that our
121 approach to generating double hu-mice is reproducible and able to create hu-mice with unique
122 16S rRNA gene profiles based on the individual human fecal donor.

123

124 **Gut microbiomes of double hu-mice have increased levels of alpha diversity compared to hu-**
125 **mice.**

126 Due to the highly reciprocal nature of the gut microbiome and immune system, we
127 hypothesized that highly immunodeficient mice, such as NSG, would have low pre-existing gut
128 microbiome diversity, especially when the mice were housed under SPF conditions with limited
129 exposure to outside sources of microbes. We tested this hypothesis and found that the gut
130 microbial diversity of double hu-mice with a functional immune system significantly increased
131 to the levels observed in our human donor samples compared to hu-mice. Several alpha
132 diversity measurements confirmed that hu-mice had very low measures of alpha diversity
133 compared to our human donor samples (Fig. 3). However, after engraftment, double hu-mice
134 had increased species richness compared to hu-mice ($P < .001$) and did not differ significantly
135 from the human donor samples (Fig. 3a). Further, the Shannon index values of the human
136 donor samples were significantly higher than hu-mice ($P < .05$) but were not significantly
137 different from the double hu-mice samples. Double hu-mice had increased Simpson index
138 values compared to hu-mice, but the human donor samples were significantly higher than both
139 the double hu-mice ($P < .05$) and hu-mice ($P < .05$). As expected, samples taken during antibiotic
140 treatment had the lowest measures of all three diversity metrics tested. Alpha diversity metrics

141 were also measured based on the human donor sample engrafted (Supplemental Figure –
142 Alpha_Diversity.pdf). Double hu-mice engrafted after 14 days of antibiotics (donor 65 cohorts 1
143 & 2, donor mix) had higher levels of alpha diversity compared to double hu-mice engrafted
144 after only 7 days of antibiotics (donors 74 & 82). Overall, double hu-mice had increased alpha
145 diversity compared to hu-mice that was more similar to the levels observed in the human donor
146 samples. The shorter antibiotic treatment duration (7 days versus 14 days) was associated with
147 lower alpha diversity measurements in double hu-mice engrafted with human donors 74 or 82.

148

149 **The relative abundance of gut bacteria in double hu-mice is similar to that found in human**
150 **donor samples.**

151 We next hypothesized that if bacteria from the human donors were successfully
152 engrafted into double hu-mice, then we would see more taxonomic similarities between human
153 donor gut microbiome profiles and double hu-mice versus hu-mice. Several differences were
154 observed in the relative abundances of double hu-mice based on the length of antibiotic
155 treatment, the human fecal donor sample engrafted, and mouse cohort (Supplemental Figure –
156 Relative_Abundances.pdf). At the Phylum level, both double hu-mice and hu-mice samples
157 were largely represented by *Actinobacteria*, *Bacteroidetes*, *Firmicutes*, and *Verrucomicrobia*.
158 Interestingly, we found that hu-mice had high proportions of *Verrucomicrobia* that remained
159 high even after antibiotic treatment and engraftment with human donor samples that had low
160 abundances of *Verrucomicrobia*. At the Family level, hu-mice samples had a higher relative
161 abundance of *S24-7* than double hu-mice and human donor samples (Fig. 4). Both hu-mice and
162 double hu-mice samples had higher relative abundances of *Lactobacillaceae* and

163 *Verrucomicrobiaceae* than human donor samples. The human donor and double hu-mice
164 samples had higher relative abundances of *Bacteroidaceae* than hu-mice samples. The human
165 donor samples also had a much higher relative abundance of *Lachnospiraceae*.

166 We next compared the taxonomic differences between the microbiomes using Kruskal-
167 Wallis testing with FDR adjusted P values below .05 (Supplemental File – KW_Testing.xlsx). We
168 found 195 significant differences between the hu-mice and human donor samples and 170
169 significant differences between hu-mice and double hu-mice. However, only 108 significant
170 differences were observed between double hu-mice and human donor samples. Both the
171 human donor and double hu-mice samples had significantly higher relative abundances of the
172 genus *Bacteroides*, while hu-mice had a significantly higher relative abundance of the family
173 *S24-7*. Human donor samples had a higher relative abundance of the Phylum *Firmicutes*
174 compared to both hu-mice and double hu-mice. Human donor samples had lower relative
175 abundances of the class *Bacilli* and family *Lactobacillaceae* compared to both hu-mice and
176 double hu-mice. Human donor samples also had a higher relative abundance of the class
177 *Clostridia* than both hu-mice and double hu-mice samples. Significant differences found within
178 this class were the family *Lachnospiraceae*, genus *Blautia*, genus *Roseburia*, family
179 *Ruminococcaceae*, genus *Ruminococcus*, and species *Faecalibacterium prausnitzii*. Some of
180 these taxa do increase in abundance in double hu-mice as compared to hu-mice, as observed
181 with significant differences in the genus *Blautia* and genus *Ruminococcaceae*. Levels of the
182 species *Akkermansia muciniphila* are significantly higher in hu-mice and double hu-mice
183 samples compared to human donor samples. However, double hu-mice have significantly less
184 relative abundance of this species than hu-mice samples.

185 To further determine differences in relative abundances among microbiomes from the
186 various treatments, we used Linear discriminant analysis Effect Size (LEfSe) with a P value < .05
187 and LDA score > 2 (Supplemental File – LefSe.xlsx)[23]. Taxa with LDA scores higher than 4
188 were plotted to show significant differences between double hu-mice and human donor
189 samples and double hu-mice and hu-mice samples (Fig. 5). Human donor samples were
190 associated with higher relative abundances of several types of *Clostridia* including
191 *Lachnospiraceae*, *Blautia*, *Coprococcus*, *Roseburia*, *Facalibacterium*, and *Ruminococcus*
192 compared to double hu-mice, while double hu-mice samples were associated with *Lactobacillus*
193 and *Akkermansia muciniphila* (Fig. 5a). Double hu-mice were associated with higher relative
194 abundances of *Bacteroides* and several types of *Clostridia* including *Blautia*, *Coprococcus*, and
195 *Ruminococcaceae*, while hu-mice samples were associated with S24-7 and *Mogibacteriaceae*
196 (Fig. 5b). By characterizing the relative bacterial abundance in double hu-mice, we
197 demonstrated that certain taxa, like members of *Bacteroides*, readily engrafted while others
198 such as *Clostridia* were more difficult to transplant. Further, several species such as those found
199 in the phylum *Verrucomicrobia* were highly prevalent in hu-mice, and antibiotic treatment
200 followed by fecal transplant did not fully diminish or replace this population based on relative
201 abundances. Altogether, these results demonstrate that engraftment of human donor samples
202 significantly changed the taxonomic profile of double hu-mice and that their human-like gut
203 microbiomes were statistically more similar to human donor profiles compared to hu-mice.
204
205 **The engrafted human-like gut microbiome in double hu-mice is stable.**

206 To evaluate the stability of the engrafted human-like gut microbiome in double hu-mice
207 after fecal transplant, the proportion of shared amplicon sequence variants (ASVs) with the
208 human donor sample was calculated (Fig. 6). After engraftment, double hu-mice had increased
209 proportions of shared ASVs with their respective human donor samples, and those proportions
210 remained higher than pre-treatment and control levels for the duration of the study. The first
211 cohort of double hu-mice engrafted with human donor 65 had an average shared ASV
212 proportion of 13.70% after transplant, while the pre-treatment samples had 1.06% and control
213 samples levels had 1.42% (Fig. 6a). This increased proportion of shared ASVs was maintained
214 for the duration of the study, up to 14 weeks post-transplant. A second cohort of double hu-
215 mice engrafted with human donor 65 was created and a similar increase in the proportion of
216 shared ASVs was observed (Fig. 6b). The average proportion of shared ASVs was 17.65% post-
217 transplant, while the pre-treatment samples had 2.60% and the control samples had 0.96%.
218 This increased proportion of shared ASVs was maintained for the duration of the study, up to
219 14.5 weeks post-transplant. Double hu-mice transplanted with the mixture of all three human
220 donors had an average shared ASV proportion of 10.91% after transplant, while the pre-
221 treatment samples had 0.31% and the control samples had 0.61% (Fig. 6d).

222 The proportion of shared ASVs was then calculated for cohorts of double hu-mice only
223 treated with 7 days of antibiotics prior to fecal transplant. Double hu-mice engrafted with
224 human donor 74 had an average shared ASV proportion of 11.85% after transplant, while the
225 pre-treatment samples had 1.02% and the control samples had 0.86% (Fig. 6c). Double hu-mice
226 transplanted with human donor 82 had an average shared ASV proportion of 10.56% after

227 transplant, while the pre-treatment samples had 1.33% and the control samples had 0.95% (Fig.
228 6c).

229 To further evaluate the stability of the engrafted human-like microbiome after
230 transplant into double hu-mice, the contributions of the human donor and pre-treatment
231 sample to the post-transplant samples were determined using SourceTracker (Fig. 7)[24]. The
232 first cohort of mice transplanted with human donor 65 had an average donor contribution
233 percentage of 18.76% after transplant, while the pre-treatment samples had 0.00% and the
234 control samples had 0.05% (Fig. 7a). At the final time point collected at 14 WPT, the donor
235 contribution was consistent at 18.10%. The second cohort of mice transplanted with human
236 donor 65 had an average donor contribution percentage of 29.01% after transplant, while the
237 pre-treatment and controls samples had no donor contribution (Fig. 7b). The donor
238 contribution percentage was 34.10% at 14.5 WPT, thus demonstrating the stable engraftment
239 of donor bacteria. Double hu-mice engrafted with donor 74 had an average donor contribution
240 percentage of 12.71% after transplant, while the pre-treatment samples had 0.00% and the
241 control samples had 0.00% (Fig. 7c). At the final time point collected at 6 WPT, the average
242 donor contribution was 18.75%.

243 The SourceTracker algorithm was unable to clearly distinguish donor 82 contributions as
244 both pre-treatment and control samples were assigned high human donor contribution
245 percentages. Mice transplanted with human donor 82 had an average donor contribution
246 percentage of 10.18% after transplant, while the pre-treatment samples had 11.95% and the
247 control samples had 20.62% (Fig. 7c). SourceTracker also assigned very high donor contribution
248 percentages to the pre-treatment and control samples in the study of double hu-mice

249 transplanted with a mixture of all three human donors. Mice transplanted with the mixture of
250 all three human donors had an average donor contribution percentage of 14.88% after
251 transplant, while the pre-treatment samples had 21.04% and the control samples had 15.89%
252 (Fig. 7d).

253 The high donor contribution percentages of donor 82 to the pre-treatment and control
254 samples originated from an ASV with taxonomic assignment to *Akkermansia muciniphila*. This
255 ASV was highly abundant in both hu-mice and double hu-mice and was much more prevalent in
256 human donor 82 and the mixed donor sample compared to donors 65 or 74. To get a more
257 accurate account of the stability of the human-like gut microbiome in post-transplant samples,
258 we removed this ASV that was resulting in false positive donor contributions and once again
259 used SourceTracker (Supplemental Figure – SourceTracker_82_Mix.pdf). After the removal of
260 the ASV, the double hu-mice engrafted with human donor 82 had an average donor
261 contribution percentage of 12.64% after transplant and double hu-mice engrafted with the
262 mixture of all three human donors had an average donor contribution percentage of 18.11%
263 after transplant, while all pre-treatment control samples were at 0.00%. Using both a
264 percentage of shared ASVs and SourceTracker, we have demonstrated that double hu-mice had
265 a stable human-like gut microbiome for the duration of the study, up to 14.5 weeks post-
266 transplant.

267

268 **Double hu-mice have increased human-like predicted metagenome functional content.**

269 In addition to evaluating microbiome classification, we also sought to assess the
270 functional capacity of the microbiomes in double hu-mice. PICRUSt was used to predict the

271 metagenome functional content from the 16S rRNA data after ASV inference [25], and the
272 predicted KO features were graphed using both NMDS and PCoA plots (Fig. 8). Many of the
273 double hu-mice samples clustered closer to the human donor samples than the hu-mice
274 samples (Fig. 8a & 8b). When color-coded by donor and cohort, the microbiomes that clustered
275 closest to the human donor samples belonged to mice from the second cohort of double hu-
276 mice generated by engrafting bacteria from human donor 65 (Fig 8c & 8d). Similarly, several
277 samples from the other double hu-mice cohorts also separated themselves from the hu-mice
278 cluster and were closer to the human donor samples. (Fig. 8c & 8d).

279 We next tested for differences of each predicted KO feature among the three different
280 groups of mice (Supplemental File – KO_Significant_Differences.xlsx). In total, there were 4,513
281 non-zero predicted KO features. Using Kruskal-Wallis testing and an FDR adjusted p-value of <
282 0.05, we found 35.54% (1,604/4,513) significantly different predicted KO features between hu-
283 mice and human donor samples. There were 39.09% (1,764/4,513) significantly different
284 predicted KO features between double hu-mice and hu-mice samples. However, when we
285 compared double hu-mice and the human donor samples, there were only 1.35% (61/4,513)
286 significantly different predicted KO features. To clarify what functional aspects were missing
287 from the double hu-mice gut microbiomes, we determined the predicted ASV contribution for
288 each of the 61 significantly different KO features between the double hu-mice and human
289 donor samples (Supplemental File – KO_Metagenome_Contribution.xlsx). This analysis provided
290 insight into which functionally significant bacteria were not successfully engrafted from the
291 human donor samples to the double hu-mice. A total of 95 ASVs with 73 unique taxonomic
292 assignments were found to contribute to the 61 significantly different KO features

293 (Supplemental Figure – KO_Contributions.pdf). Family level taxa with the highest levels of
294 contribution included *Actinomycetaceae* (10.46%), *Bifidobacteriaceae* (8.76%),
295 *Streptococcaceae* (20.74%), *Lachnospiraceae* (23.95%), and *Peptococcaceae* (8.66%).
296 *Bifidobacterium adolescentis* was the highest contributing species (7.85%), and the highest
297 contributing ASV (13.01%) had the taxonomic assignment of an unclassified *Streptococcus*
298 species. Collectively, these analyses demonstrate that the predicted functional capacity of
299 double hu-mice is more similar to human donor samples compared to hu-mice.

300

301 **Discussion**

302 The goal of this study was to investigate the establishment and stability of an engrafted
303 human gut microbiome after antibiotic pre-treatment in hu-mice. We call these mice double
304 hu-mice as they have both a functional human immune system and human bacterial gut
305 microbiomes similar to human donor samples. Our approach created highly reproducible and
306 donor-specific human-like gut microbiomes across multiple cohorts of double hu-mice. Further,
307 we showed that double hu-mice had increased measures of diversity and increased functional
308 capacity compared to hu-mice. The engrafted human-like gut microbiomes were also stable for
309 the duration of the study, up to 14.5 weeks post-transplant. Further, we demonstrated that the
310 predicted functional capacity of double hu-mice is also more similar to the human donor
311 samples than hu-mice.

312 One of the most significant aspects of the study was that the double hu-mice had gut
313 microbiome profiles that were unique to the human donor engrafted. Each of the 4 different
314 donor samples resulted in a distinct population of double hu-mice resembling the human

315 donor. Double hu-mice create a huge opportunity for implementing personalized medicine and
316 translational research. Potential applications for double hu-mice include testing for
317 personalized responses of patient microbiomes to drug regimens, therapies, or dietary
318 interventions. These mice could also be used to identify mechanisms underlying observations
319 from human studies establishing a connection between the gut microbiome and disease.

320 In this study, we created a cohort of double hu-mice by engrafting a mixture of all three
321 human donors to create an ‘un-biased’ human gut microbiome profile. Further study is needed
322 to determine whether a mixed sample is beneficial in creating an un-biased human-like profile
323 or if mixing samples creates an un-natural or unstable community of gut bacteria after
324 engraftment. It may be advantageous to use a mixture of fecal samples derived from a large
325 population to determine the broad impact of different treatments or diets to the human gut
326 microbiome. This un-biased mix of a large population of donors could be used to add additional
327 information to double hu-mice generated with individual donor profiles.

328 We found that double hu-mice had increased measures of alpha diversity compared to
329 hu-mice. Several studies have highlighted the importance of microbiome diversity within the
330 gut and have linked low gut microbiome diversity with several disease conditions[26, 27]. While
331 not all low diversity conditions are detrimental, specifically when there is enrichment of
332 potentially beneficial bacteria through prebiotic or probiotic treatment, the low pre-existing
333 diversity found within the hu-mice was far below the levels observed in our human donor
334 samples. After engraftment, the double hu-mice had increased levels of alpha diversity and
335 maybe more importantly, had increased predicted functional capacities. This increased diversity

336 may also offer a more realistic gut environment as it allows for diverse reciprocal interactions
337 with the engrafted human immune system.

338 We also found that the engrafted human-like microbiome was very stable in our model
339 for the length of the study, up to 14.5 weeks after transplant. We used several methods to
340 determine the engraftment level and stability of the gut microbiome after transplant and found
341 no reversion to the pre-existing murine profile. This stability allows study of the role of the gut
342 microbiome in many human diseases such as HIV-1 and cancer. One outstanding question is
343 whether the unique presence of human immune cells plays a role in stabilizing or enhancing
344 engraftment of the human-like gut microbiome in our model compared to other non-
345 humanized mouse models. Our data showed no reversion to the pre-existing murine gut
346 microbiome profile, perhaps due to some enhanced stability or selection by the reconstituted
347 human immune system. Further studies are needed to determine the relationship between the
348 engrafted gut microbiome and human immune system.

349 Many different methods and antibiotic regimens have been used for preconditioning of
350 mice prior to fecal transplantation[28-30]. Different combinations and durations of antibiotic
351 treatments may increase the efficiency of the fecal transplant into the host[29]. While the
352 combination of Metronidazole, Ampicillin, Neomycin, and Vancomycin is widely used due to its
353 broad spectrum of bacterial targets, the best methods are still being investigated. We found
354 that the very rigorous method of gavaging antibiotics twice daily for 14 days used by Hintze et
355 al. was too invasive for our NSG hu-mice and resulted in increased mortality[31]. Providing the
356 antibiotics in the drinking water proved to be less stressful with improved health and survival of

357 the mice. Meanwhile, we also found that 14 days was the optimum duration of antibiotic pre-
358 treatment to generate double hu-mice.

359 As expected, there is not a complete reconstitution of the human fecal donor profile in
360 our double hu-mice due to several hypothesized reasons. There are major differences between
361 the human and mouse digestive tract including structure, function, and pH[19]. Our mice are
362 not germ-free to begin with, and the broad-spectrum antibiotic treatment can only reduce the
363 prevalence of pre-existing murine gut bacteria. There were several key differences in the
364 reconstituted mice compared to the human donors. Double hu-mice had significantly lower
365 levels of several types of *Clostridia* including *Lachnospiraceae*, *Blautia*, *Coprococcus*, *Roseburia*,
366 *Faecalibacterium*, and *Ruminococcus* compared to human donor samples. Many of these
367 bacteria are well documented to be difficult to reconstitute within germ-free and SPF mouse
368 models[20, 31, 32]. Similar to fecal transplants in humans designed to treat *C. difficile*
369 infections, the engrafted human-like gut microbiome in our double hu-mice is the result of a
370 combination of host, donor, and environmental bacteria[33]. Despite these previously known
371 limitations, our double hu-mice model reproducibly results in a donor specific, stable, human-
372 like gut microbiome in the presence of a human immune system.

373 Germ-free animals are the gold standard for studying the gut microbiome. Using germ-
374 free mice to study the impact of the gut microbiome has been well-documented[1, 20]. Germ-
375 free animal models may allow for a more complete reconstitution of a human-like gut
376 microbiome following fecal transplant, however these models often do not have human
377 immune system. Studying human immune reconstitution in hu-mice and pathogenesis of
378 human specific diseases in a gnotobiotic environment could reveal important clues about the

379 role of the gut microbiome. Nevertheless, many important mouse strains are not commercially
380 available as germ-free, including NSG mice. Several studies have also shown that gnotobiotic
381 mice may have long-lasting immune deficiencies, even after gut microbiome reconstitution[34-
382 36]. Further, working with germ-free animals requires gnotobiotic facilities and equipment that
383 is expensive and has limited availability. Lundberg et al., and Kennedy et al., nicely review the
384 advantages and disadvantages of using antibiotic-treated versus germ-free rodents for
385 microbiota transplantation studies [37, 38].

386 Our double hu-mice have the advantage of requiring only SPF housing conditions, which
387 are widely available and less expensive compared to germ-free facilities. It also does not
388 perturb the complex surgical procedures in generating BLT hu-mice because there is no need
389 for a completely germ-free environment. Our NSG mice are housed and bred under SPF
390 conditions and the diversity of their murine gut microbiota is low. Their immunodeficiency may
391 contribute to their pre-existing low diversity gut microbiome status before human fecal
392 material transplant. In a study by Zhou et al., NSG and C57BL6/J mice whose native microbiota
393 were depleted by antibiotics followed by FMT had no significant differences in diversity but did
394 observe significant differences in which species colonized[39]. A study done by Ericsson et al.
395 showed that it is easier to transfer high diversity fecal donor samples into low diversity
396 recipients, which could help to explain the success of engraftment and stability in our
397 model[30]. Many questions remain as to the best antibiotic preconditioning regimen, the timing
398 of fecal transplants, the total number of fecal transplants, the route of administration (oral
399 versus rectal), the use of antacids, and preconditioning with osmotic laxatives such as

400 polyethylene glycol, diet, and housing. Methods to optimize murine bacterial depletion along
401 with reconstitution and stability of human specific bacteria are currently being explored.

402

403 **Conclusion**

404 Here, we describe successful and stable transplantation of human fecal microbiomes
405 into immunodeficient NSG mice surgically engrafted with a functional human immune system
406 to create double hu-mice with human donor-specific human gut microbiomes. Double hu-mice
407 will be beneficial to many applications of personalized medicine to test the impact of the
408 human gut microbiome on human health and disease in the presence of a human immune
409 system.

410

411 **Methods**

412 **Generation of humanized BLT mice**

413 All methods described here were conducted as we previously reported in accordance
414 with Institutional Animal Care and Research Committee (IACUC)-approved protocols at the
415 University of Nebraska-Lincoln (UNL)[22, 40-42]. The IACUC at the University of Nebraska-
416 Lincoln (UNL) has approved two protocols related to generating and using humanized BLT (hu-
417 BLT) mice, including Double Hu-Mice. Additionally, the Scientific Research Oversight Committee
418 (SROC) at UNL has also approved the use of human embryonic stem cells and fetal tissues,
419 which are procured from the Advanced Bioscience Resources for humanized mice studies
420 (SROC# 2016—1-002).

421 Briefly, 6- to 8-week-old female NSG mice (NOD.*Cg-Prkdc^{scid}Il2rg^{tm1Wjl}*/SzJ, catalog
422 number 005557; (Jackson Laboratory) were housed and maintained in individual microisolator
423 cages in a rack system capable of managing air exchange with prefilters and HEPA filters. Room
424 temperature, humidity, and pressure were controlled, and air was also filtered. Mice were fed
425 irradiated Teklad global 14% protein rodent chow (Teklad 2914) and were given autoclaved
426 acidified drinking water. The second cohort of double hu-mice engrafted with fecal material
427 from Donor 65 were supplemented with a high calorie gel (DietGel Boost). On the day of
428 surgery, mice received whole-body irradiation at the dose of 12 cGy/gram of body weight with
429 the RS200 X-ray irradiator (RAD Source Technologies, Inc., GA) and were then implanted with
430 one piece of human fetal thymic tissue fragment sandwiched between two pieces of human
431 fetal liver tissue fragments within the murine left renal capsule. Within 6 hours of surgery, mice
432 were injected via the tail vein with 1.5×10^5 to 5×10^5 CD34⁺ hematopoietic stem cells isolated
433 from human fetal liver tissues. Human fetal liver and thymus tissues were procured from
434 Advanced Bioscience Resources (Alameda, CA). After 9 to 12 weeks, human immune cell
435 reconstitution in peripheral blood was measured by a fluorescence-activated cell sorter (FACS)
436 Aria II flow cytometer (BD Biosciences, San Jose, CA) using antibodies against mCD45-APC,
437 hCD45-FITC, hCD3-PE, hCD19-PE/Cy5, hCD4-Alexa 700, and hCD8-APC-Cy7 (catalog numbers
438 103111, 304006, 300408, 302209, 300526, and 301016, respectively; BioLegend, San Diego,
439 CA). Raw data were analyzed with FlowJo (version 10.0; FlowJo LLC, Ashland, OR). All mice used
440 in this study had high levels of human immune cell reconstitution with an average of 85%
441 hCD45+ cells in peripheral blood 10 weeks post-surgery. The mice were randomly assigned into
442 experimental groups with similar immune reconstitution levels.

443

444 **Antibiotic treatment**

445 A broad-spectrum antibiotic cocktail was prepared fresh daily consisting of
446 Metronidazole (1 g/L), Neomycin (1 g/L), Vancomycin (0.5 g/L), and Ampicillin (1 g/L). The
447 antibiotic cocktail was given to the mice ad libitum in the drinking water along with grape
448 flavored Kool-Aid to improve palatability. Control group mice were given only grape flavored
449 Kool-Aid in the drinking water. During antibiotic treatment, cages were changed daily to limit
450 re-inoculation of pre-existing bacteria to the mice due to their coprophagic behavior.
451 Antibiotics were given for 14 days for double hu-mice reconstituted with Donor 65 and Donor
452 Mix and for 7 days in double hu-mice reconstituted with Donor 74 and Donor 82. Mice in the
453 Pilot Study were given antibiotics via oral gavage. Mice were first given three days of anti-fungal
454 Amphotericin B treatment (1 mg/kg) twice daily via oral gavage. Mice were then given the
455 antibiotic cocktail along with Amphotericin B via twice daily via oral gavage. After 4 days of
456 treatment, the Amphotericin B was stopped due to toxicity concerns and after 10 days of
457 treatment oral gavage was reduced to once daily. Post-antibiotic treatment, mice were given
458 autoclaved non-acidified deionized drinking water.

459 During the first few days of antibiotic treatment, the mice lost a considerable amount of
460 body weight (10-20%). The weight loss plateaued at 3-4 days and remained steady for the
461 remainder of antibiotic treatment. Body weight was carefully monitored during this time and if
462 needed, mice were treated with Intraperitoneal (IP) injections of Ringer's solution to mitigate
463 any effects of dehydration. After fecal transplant, the mice began to regain weight and returned
464 to their pre-existing weight within 2 weeks post-transplant. During antibiotic treatment, there

465 was a large reduction in spleen size and a large increase in cecum size compared to controls.
466 This is similar to the morphology observed in germ-free mice, providing further evidence for the
467 efficacy of the antibiotic regimen[35].

468

469 **Donor samples and Fecal transplant**

470 At 24 and 48 hours after the completion of antibiotic pre-treatment, mice were given
471 200 ul of human fecal material via oral gavage. OpenBiome supplied 3 FMT Upper Delivery
472 Microbiota Preparations from 3 different healthy human donors (Donor 65, Donor 74, Donor
473 82). Samples were thawed once before fecal transplant to aliquot the samples within an
474 anaerobic chamber. During this step, an equal portion of each of the samples were mixed
475 together to create an unbiased human donor sample (Donor Mix). 16S rRNA sequencing data
476 on the three donors was also supplied by OpenBiome (Supplementary data).

477

478 **Mouse fecal collection and DNA extraction**

479 Individual mice were placed into autoclaved paper bags within a biosafety hood until
480 fresh fecal samples were produced. Fecal samples were stored in 1.5 ml Eppendorf tubes at -80
481 °C until DNA extraction. DNA was extracted from the fecal samples using the
482 phenol:chloroform:isoamyl alcohol with bead beating method described previously [43]. Briefly,
483 fecal samples were washed three times with 1 ml PBS buffer (pH 7). After the addition of 750 ul
484 of lysis buffer, samples were transferred to tubes containing 300 mg of autoclaved 0.1 mm
485 zirconia/silica beads (Biospec). 85 ul of 10% SDS solution and 40 ul of Proteinase K (15mg/ml,
486 MC500B Promega) were added and samples were incubated for 30 minutes at 60° C. 500 ul of

487 Phenol:Chloroform:Isoamyl alcohol (25:24:1) was added and then samples were vortexed.
488 Samples were then put into a bead beater (Mini-beadbeater 16 Biospec) for 2 minutes to
489 physically lyse the cells. The upper phase of the sample was collected and an additional 500ul of
490 Phenol:Chloroform:Isoamyl alcohol (25:24:1) was added. After samples were vortexed and spun
491 down, the DNA in the upper phase was further purified twice with 500 ul of
492 Phenol:Chloroform:Isoamyl alcohol (25:24:1). and was then precipitated with 100% Ethanol (2.5
493 x volume of sample) and 3M Sodium acetate (.1 x volume of sample) overnight at -20° C.
494 Samples are then centrifuged and dried at room temperature. DNA was resuspended in 100 ul
495 of Tris-Buffer (10mM, pH8) and stored at -20° C. DNA samples were quality checked by
496 nanodrop (ND-1000 Nanodrop) .

497

498 **16S rRNA gene sequencing**

499 16S rRNA gene sequencing was performed at the University of Nebraska Medical Center
500 Genomics Core Facility using xxx (detailed Illumina instrument here). DNA normalization and
501 library prep were performed followed by V3-V4 16S rRNA amplicon gene sequencing using a
502 MiSeqV2 (Illumina) The following primer sequences were used: (Primer sequences: Forward
503 Primer = 5'
504 TCGTCGGCAGCGTCAGATGTGTATAAGAGACAGCCTACGGGNGGCWGCAG 16S Amplicon PCR
505 Reverse Primer = 5'
506 GTCTCGTGGGCTCGGAGATGTGTATAAGAGACAGGACTACHVGGGTATCTAATCC

507 Illumina overhangs: Forward overhang: 5'
508 TCGTCGGCAGCGTCAGATGTGTATAAGAGACAG-[locusspecific sequence] Reverse overhang: 5'
509 GTCTCGTGGGCTCGGAGATGTGTATAAGAGACAG-[locusspecific sequence]).

510

511 **Generation of the amplicon sequence variant table and data analysis**

512 Illumina-sequenced paired-end fastq files were demultiplexed by sample and barcodes
513 were removed by the sequencing facility. The University of Nebraska Holland Computer Center
514 Crane cluster was used to run the DADA2 v1.8 R package in order to generate an amplicon
515 sequence variant (ASV) table[44]. An example of the script used to generate the ASV table is
516 provided in the supplementary materials. The DADA2 pipeline was performed as follows,
517 sequences were filtered and trimmed during which any remaining primers, adapters, or linkers
518 were also removed. The sequencing error rates were estimated using a random subset of the
519 data. Dereplication of the data combined all identical sequencing reads into unique sequences
520 with a corresponding abundance. The core sample inference algorithm was then applied to the
521 dereplicated data. The forward and reverse reads were then joined to create the full denoised
522 sequences and an initial ASV table was generated. Any sequences outside the expected length
523 for the V3-V4 amplicon were then filtered from the table. Chimeric sequences were then
524 removed and a final ASV table was generated. Taxonomy was assigned using the Greengenes
525 13.8 database and RDP Classifier with a minimal confidence score of 0.80[45, 46].

526

527 **Data analysis**

528 Analysis was performed using R package mctoolsr (<https://github.com/leffj/mctoolsr/>).

529 and samples were rarified to 13,000 ASVs for downstream analysis. Additional testing of
530 differences between groups was performed using LEfSe[23]. SourceTracker was used to
531 evaluate the stability of the transferred donor microbiome in the double hu-mice[24].
532 GraphPad Prism 5 were used to create some figures. DADA2 generated ASVs were used to
533 predict the functional metagenome capacity using PICRUSt[25] via the following pipeline
534 (https://github.com/vmaffei/dada2_to_picrust).

535

536 **Data availability**

537 The datasets generated during the current study are available in the NCBI SRA repository,
538 [<https://www.ncbi.nlm.nih.gov/bioproject/PRJNA507247>].

539

540

541

542 **References**

- 543 1. Turnbaugh PJ, Ley RE, Mahowald MA, Magrini V, Mardis ER, Gordon JI: **An obesity-**
544 **associated gut microbiome with increased capacity for energy harvest.** *Nature* 2006,
545 **444:1027-1031.**
- 546 2. Gopalakrishnan V, Spencer CN, Nezi L, Reuben A, Andrews MC, Karpinets TV, Prieto PA,
547 Vicente D, Hoffman K, Wei SC, et al: **Gut microbiome modulates response to anti-PD-1**
548 **immunotherapy in melanoma patients.** *Science* 2018, **359:97-103.**
- 549 3. Routy B, Le Chatelier E, Derosa L, Duong CPM, Alou MT, Daillere R, Fluckiger A,
550 Messaoudene M, Rauber C, Roberti MP, et al: **Gut microbiome influences efficacy of**
551 **PD-1-based immunotherapy against epithelial tumors.** *Science* 2018, **359:91-+.**
- 552 4. Clemente JC, Manasson J, Scher JU: **The role of the gut microbiome in systemic**
553 **inflammatory disease.** *Bmj-British Medical Journal* 2018, **360.**
- 554 5. Qin J, Li R, Raes J, Arumugam M, Burgdorf KS, Manichanh C, Nielsen T, Pons N, Levenez
555 F, Yamada T, et al: **A human gut microbial gene catalogue established by metagenomic**
556 **sequencing.** *Nature* 2010, **464:59-65.**
- 557 6. Kau AL, Ahern PP, Griffin NW, Goodman AL, Gordon JI: **Human nutrition, the gut**
558 **microbiome and the immune system.** *Nature* 2011, **474:327-336.**

- 559 7. Hooper LV, Littman DR, Macpherson AJ: **Interactions Between the Microbiota and the**
560 **Immune System.** *Science* 2012, **336**:1268-1273.
- 561 8. Maynard CL, Elson CO, Hatton RD, Weaver CT: **Reciprocal interactions of the intestinal**
562 **microbiota and immune system.** *Nature* 2012, **489**:231-241.
- 563 9. Simpson-Abelson MR, Sonnenberg GF, Takita H, Yokota SJ, Conway TF, Kelleher RJ,
564 Shultz LD, Barcos M, Bankert RB: **Long-term engraftment and expansion of tumor-**
565 **derived memory T cells following the implantation of non-disrupted pieces of human**
566 **lung tumor into NOD-scid IL2R gamma(null) mice.** *Journal of Immunology* 2008,
567 **180**:7009-7018.
- 568 10. Bankert RB, Balu-lyer SV, Odunsi K, Shultz LD, Kelleher RJ, Barnas JL, Simpson-Abelson
569 M, Parsons R, Yokota SJ: **Humanized Mouse Model of Ovarian Cancer Recapitulates**
570 **Patient Solid Tumor Progression, Ascites Formation, and Metastasis.** *Plos One* 2011, **6**.
- 571 11. Vudattu NK, Waldron-Lynch F, Truman LA, Deng SY, Preston-Hurlburt P, Torres R,
572 Raycroft MT, Mamula MJ, Herold KC: **Humanized Mice as a Model for Aberrant**
573 **Responses in Human T Cell Immunotherapy.** *Journal of Immunology* 2014, **193**:587-596.
- 574 12. Whitfield-Larry F, Young EF, Talmage G, Fudge E, Azam A, Patel S, Largay J, Byrd W, Buse
575 J, Calikoglu AS, et al: **HLA-A2 Matched Peripheral Blood Mononuclear Cells From Type 1**
576 **Diabetic Patients, but Not Nondiabetic Donors, Transfer Insulinitis to NOD-scid/gamma**
577 **c(null)/HLA-A2 Transgenic Mice Concurrent With the Expansion of Islet-Specific CD8(+)**
578 **T cells.** *Diabetes* 2011, **60**:1726-1733.
- 579 13. Yi GH, Xu XQ, Abraham S, Petersen S, Guo H, Ortega N, Shankar P, Manjunath N: **A DNA**
580 **Vaccine Protects Human Immune Cells against Zika Virus Infection in Humanized Mice.**
581 *Ebiomedicine* 2017, **25**:87-94.
- 582 14. Stary G, Olive A, Radovic-Moreno AF, Gondek D, Alvarez D, Basto PA, Perro M, Vrbanac
583 VD, Tager AM, Shi JJ, et al: **A mucosal vaccine against Chlamydia trachomatis generates**
584 **two waves of protective memory T cells.** *Science* 2015, **348**.
- 585 15. Sun ZF, Denton PW, Estes JD, Othieno FA, Wei BL, Wege AK, Melkus MW, Padgett-
586 Thomas A, Zupancic M, Haase AT, Garcia JV: **Intrarectal transmission, systemic**
587 **infection, and CD4(+) T cell depletion in humanized mice infected with HIV-1.** *Journal*
588 *of Experimental Medicine* 2007, **204**:705-714.
- 589 16. Wang LX, Kang GB, Kumar P, Lu WX, Li Y, Zhou Y, Li QS, Wood C: **Humanized-BLT mouse**
590 **model of Kaposi's sarcoma-associated herpesvirus infection.** *Proceedings of the*
591 *National Academy of Sciences of the United States of America* 2014, **111**:3146-3151.
- 592 17. Ernst W: **Humanized mice in infectious diseases.** *Comparative Immunology*
593 *Microbiology and Infectious Diseases* 2016, **49**:29-38.
- 594 18. Xiao L, Feng Q, Liang SS, Sonne SB, Xia ZK, Qiu XM, Li XP, Long H, Zhang JF, Zhang DY, et
595 al: **A catalog of the mouse gut metagenome.** *Nature Biotechnology* 2015, **33**:1103-+.
- 596 19. Nguyen TLA, Vieira-Silva S, Liston A, Raes J: **How informative is the mouse for human**
597 **gut microbiota research?** *Disease Models & Mechanisms* 2015, **8**:1-16.
- 598 20. Turnbaugh PJ, Ridaura VK, Faith JJ, Rey FE, Knight R, Gordon JI: **The Effect of Diet on the**
599 **Human Gut Microbiome: A Metagenomic Analysis in Humanized Gnotobiotic Mice.**
600 *Science Translational Medicine* 2009, **1**.
- 601 21. Hazenberg MP, Bakker M, Verschoor-Burggraaf A: **Effects of the human intestinal flora**
602 **on germ-free mice.** *J Appl Bacteriol* 1981, **50**:95-106.

- 603 22. Daharsh L ZJ, Ramer-Tait A, Li Q: **A Double Humanized BLT-mice Model Featuring a**
604 **Stable Human-Like Gut Microbiome and Human Immune System.** *Jove-Journal of*
605 *Visualized Experiments* 2019.
- 606 23. Segata N, Izard J, Waldron L, Gevers D, Miropolsky L, Garrett WS, Huttenhower C:
607 **Metagenomic biomarker discovery and explanation.** *Genome Biol* 2011, **12**:R60.
- 608 24. Knights D, Kuczynski J, Charlson ES, Zaneveld J, Mozer MC, Collman RG, Bushman FD,
609 Knight R, Kelley ST: **Bayesian community-wide culture-independent microbial source**
610 **tracking.** *Nat Methods* 2011, **8**:761-763.
- 611 25. Langille MG, Zaneveld J, Caporaso JG, McDonald D, Knights D, Reyes JA, Clemente JC,
612 Burkepille DE, Vega Thurber RL, Knight R, et al: **Predictive functional profiling of**
613 **microbial communities using 16S rRNA marker gene sequences.** *Nat Biotechnol* 2013,
614 **31**:814-821.
- 615 26. Willing BP, Dicksved J, Halfvarson J, Andersson AF, Lucio M, Zheng Z, Jarnerot G, Tysk C,
616 Jansson JK, Engstrand L: **A Pyrosequencing Study in Twins Shows That Gastrointestinal**
617 **Microbial Profiles Vary With Inflammatory Bowel Disease Phenotypes.**
618 *Gastroenterology* 2010, **139**:1844-U1105.
- 619 27. Chang JY, Antonopoulos DA, Kalra A, Tonelli A, Khalife WT, Schmidt TM, Young VB:
620 **Decreased diversity of the fecal microbiome in recurrent Clostridium difficile-**
621 **associated diarrhea.** *Journal of Infectious Diseases* 2008, **197**:435-438.
- 622 28. Reikvam DH, Erofeev A, Sandvik A, Grcic V, Jahnsen FL, Gaustad P, McCoy KD,
623 Macpherson AJ, Meza-Zepeda LA, Johansen FE: **Depletion of murine intestinal**
624 **microbiota: effects on gut mucosa and epithelial gene expression.** *PLoS One* 2011,
625 **6**:e17996.
- 626 29. Staley C, Kaiser T, Beura LK, Hamilton MJ, Weingarden AR, Bobr A, Kang J, Masopust D,
627 Sadowsky MJ, Khoruts A: **Stable engraftment of human microbiota into mice with a**
628 **single oral gavage following antibiotic conditioning.** *Microbiome* 2017, **5**.
- 629 30. Ericsson AC, Personett AR, Turner G, Dorfmeier RA, Franklin CL: **Variable Colonization**
630 **after Reciprocal Fecal Microbiota Transfer between Mice with Low and High Richness**
631 **Microbiota.** *Frontiers in Microbiology* 2017, **8**:1-13.
- 632 31. Hintze KJ, Cox JE, Rompato G, Benninghoff AD, Ward RE, Broadbent J, Lefevre M: **Broad**
633 **scope method for creating humanized animal models for animal health and disease**
634 **research through antibiotic treatment and human fecal transfer.** *Gut Microbes* 2014,
635 **5**:183-191.
- 636 32. Wos-Oxley M, Bleich A, Oxley AP, Kahl S, Janus LM, Smoczek A, Nahrstedt H, Pils MC,
637 Taudien S, Platzer M, et al: **Comparative evaluation of establishing a human gut**
638 **microbial community within rodent models.** *Gut Microbes* 2012, **3**:234-249.
- 639 33. Smillie CS, Smith MB, Friedman J, Cordero OX, David LA, Alm EJ: **Ecology drives a global**
640 **network of gene exchange connecting the human microbiome.** *Nature* 2011, **480**:241-
641 244.
- 642 34. Chung HC, Pamp SJ, Hill JA, Surana NK, Edelman SM, Troy EB, Reading NC, Villablanca EJ,
643 Wang S, Mora JR, et al: **Gut Immune Maturation Depends on Colonization with a Host-**
644 **Specific Microbiota.** *Cell* 2012, **149**:1578-1593.

- 645 35. Smith K, McCoy KD, Macpherson AJ: **Use of axenic animals in studying the adaptation**
646 **of mammals to their commensal intestinal microbiota.** *Seminars in Immunology* 2007,
647 **19**:59-69.
- 648 36. Hansen CHF, Nielsen DS, Kverka M, Zakostelska Z, Klimesova K, Hudcovic T, Tlaskalova-
649 Hogenova H, Hansen AK: **Patterns of Early Gut Colonization Shape Future Immune**
650 **Responses of the Host.** *Plos One* 2012, **7**.
- 651 37. Lundberg R, Toft MF, August B, Hansen AK, Hansen CHF: **Antibiotic-treated versus**
652 **germ-free rodents for microbiota transplantation studies.** *Gut Microbes* 2016, **7**:68-74.
- 653 38. Kennedy EA, King KY, Baldrige MT: **Mouse Microbiota Models: Comparing Germ-Free**
654 **Mice and Antibiotics Treatment as Tools for Modifying Gut Bacteria.** *Frontiers in*
655 *Physiology* 2018, **9**.
- 656 39. Zhou W, Chow KH, Fleming E, Oh J: **Selective colonization ability of human fecal**
657 **microbes in different mouse gut environments.** *ISME J* 2018.
- 658 40. Li QS, Tso FY, Kang GB, Lu WX, Li Y, Fan WJ, Yuan Z, Destache CJ, Wood C: **Early Initiation**
659 **of Antiretroviral Therapy Can Functionally Control Productive HIV-1 Infection in**
660 **Humanized-BLT Mice.** *Jaids-Journal of Acquired Immune Deficiency Syndromes* 2015,
661 **69**:519-527.
- 662 41. Destache CJ, Mandal S, Yuan Z, Kang G, Date AA, Lu W, Shibata A, Pham R, Bruck P,
663 Rezich M, et al: **Topical Tenofovir Disoproxil Fumarate Nanoparticles Prevent HIV-1**
664 **Vaginal Transmission in a Humanized Mouse Model.** *Antimicrob Agents Chemother*
665 2016, **60**:3633-3639.
- 666 42. Yuan Z, Kang G, Ma F, Lu W, Fan W, Fennessey CM, Keele BF, Li Q: **Recapitulating Cross-**
667 **Species Transmission of Simian Immunodeficiency Virus SIVcpz to Humans by Using**
668 **Humanized BLT Mice.** *J Virol* 2016, **90**:7728-7739.
- 669 43. Martinez I, Wallace G, Zhang C, Legge R, Benson AK, Carr TP, Moriyama EN, Walter J:
670 **Diet-induced metabolic improvements in a hamster model of hypercholesterolemia**
671 **are strongly linked to alterations of the gut microbiota.** *Appl Environ Microbiol* 2009,
672 **75**:4175-4184.
- 673 44. Callahan BJ, McMurdie PJ, Rosen MJ, Han AW, Johnson AJ, Holmes SP: **DADA2: High-**
674 **resolution sample inference from Illumina amplicon data.** *Nat Methods* 2016, **13**:581-
675 583.
- 676 45. Wang Q, Garrity GM, Tiedje JM, Cole JR: **Naive Bayesian classifier for rapid assignment**
677 **of rRNA sequences into the new bacterial taxonomy.** *Applied and Environmental*
678 *Microbiology* 2007, **73**:5261-5267.
- 679 46. Caporaso JG, Kuczynski J, Stombaugh J, Bittinger K, Bushman FD, Costello EK, Fierer N,
680 Pena AG, Goodrich JK, Gordon JI, et al: **QIIME allows analysis of high-throughput**
681 **community sequencing data.** *Nature Methods* 2010, **7**:335-336.
- 682

683

684 **Acknowledgements**

685 We would like to thank Yanmin Wan, Guobin Kang, and Pallabi Kundu for their assistance in
686 generating BLT hu-mice. We would like to acknowledge the UNMC Genomics Core Facility who
687 receives partial support from the Nebraska Research Network In Functional Genomics NE-INBRE
688 P20GM103427-14, The Molecular Biology of Neurosensory Systems CoBRE P30GM110768, The
689 Fred & Pamela Buffett Cancer Center - P30CA036727, The Center for Root and Rhizobiome
690 Innovation (CRR) 36-5150-2085-20, and the Nebraska Research Initiative. We would like to
691 thank University of Nebraska—Lincoln Life Sciences Annex and their staff for their assistance.
692 This study is supported in part by the National Institutes of Health (NIH) Grants R01AI124804
693 (to Jarvis), R33AI122377 (Planelles), P30 MH062261-16A1 Chronic HIV Infection and Aging in
694 NeuroAIDS (CHAIN) Center (to Buch & Fox), 1R01AI111862 and R21 AI143405 to Q Li. The
695 funders had no role in study design, data collection and analysis, preparation of the manuscript
696 or decision for publication.

697

698 **Author contributions**

699 LD and QL designed the experiments and wrote the manuscript. LD performed experiments and
700 analyzed the data. ART provided input on experimental design and manuscript preparation.

701

702 **Competing interests**

703 The author(s) declare no competing interests.

704

705 **Figure Legends**

706 **Figure 1. Gut microbiomes of double hu-mice are distinct and more human-like compared to**
707 **hu-mice and feature donor specific profiles.** A) Non-metric multidimensional scaling (NMDS)
708 plot displaying double hu-mice as a distinct cluster between the human donor samples and pre-
709 treatment or untreated control hu-mice. B) Principal coordinate analysis (PCoA) plot showing
710 the double hu-mice cluster with the human donor samples distinct from the pre-treatment or
711 untreated control hu-mice. C) NMDS plot displaying human donor specific profiles in the double
712 hu-mice. D) PCoA plot showing human donor specific profiles in the double hu-mice.

713

714 **Figure 2. The gut microbiomes of double hu-mice cluster with that of human donor fecal**
715 **samples.** Dendrogram based on Bray-Curtis distances for the gut microbiome profiles of pre-
716 treatment and untreated control hu-mice (Pre-treatment or Control Hu-Mice), double hu-mice
717 (Double Hu-Mice), antibiotic treated hu-mice (Antibiotic Treated Hu-mice), and human donor
718 fecal samples (Human Donor).

719

720 **Figure 3. The gut microbiomes of double hu-mice have increased alpha diversity measures**
721 **compared to that of pre-treatment or untreated control hu-mice.** A) Species richness, B)
722 Shannon index, and C) Simpson index. Data are shown for pre-treatment or untreated control
723 hu-mice (Hu-Mice), antibiotic treated mice (Antibiotics), double hu-mice (Double Hu-Mice), and
724 human donor fecal samples (Human Donor).

725

726 **Figure 4. Comparison of relative abundance of taxa grouped by Family.** The 11 most abundant
727 taxa by relative percent abundance grouped by Family are shown for pre-treatment and

728 untreated control hu-mice (Hu-mice), double hu-mice (Double), and human fecal donor
729 samples (Donor).

730

731 **Figure 5. Engraftment of human fecal donor bacteria in double hu-mice as shown by LEfSe.** A)

732 All significant features with a linear discriminant analysis (LDA) score > 4.0 between human
733 fecal donor samples (Donor) and double hu-mice (Double). B) All significant features with an
734 LDA score > 4.0 between double hu-mice (Double) and pre-treatment or untreated control hu-
735 mice (Hu-Mice).

736

737 **Figure 6. Engraftment and stability of a human-like gut microbiome in double hu-mice as**

738 **determined by shared amplicon sequence variants (ASVs).** A) Proportion of shared ASVs with
739 the donor in the first cohort of double hu-mice created using fecal material from human donor
740 65 (Donor 65). B) Proportion of shared ASVs with donor in the second cohort of double hu-mice
741 created using fecal material from human donor 65 (Donor 65). C) Proportion of shared ASVs
742 with donor in in double hu-mice created using fecal material from human donor 74 (Donor 74)
743 or 82 (Donor 82). D) Proportion of shared ASVs with donor in double hu-mice created using a
744 mixture of fecal material from all three human donors (Donor Mix). X-axis numbers represent
745 number of weeks post fecal transplant.

746

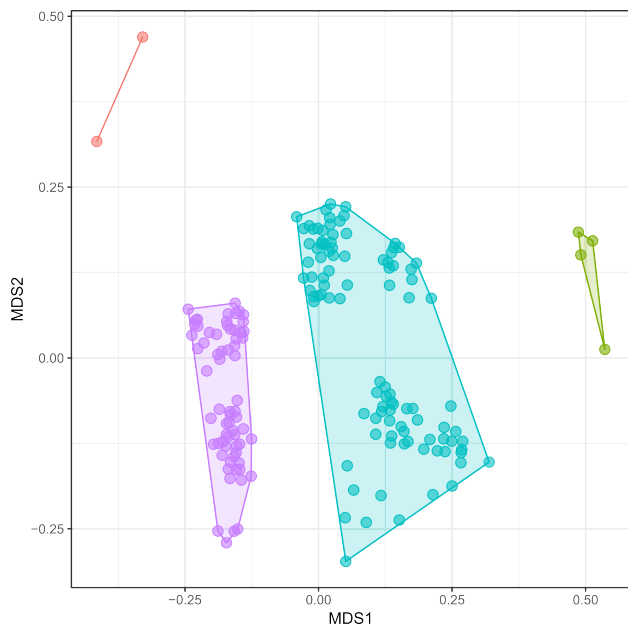
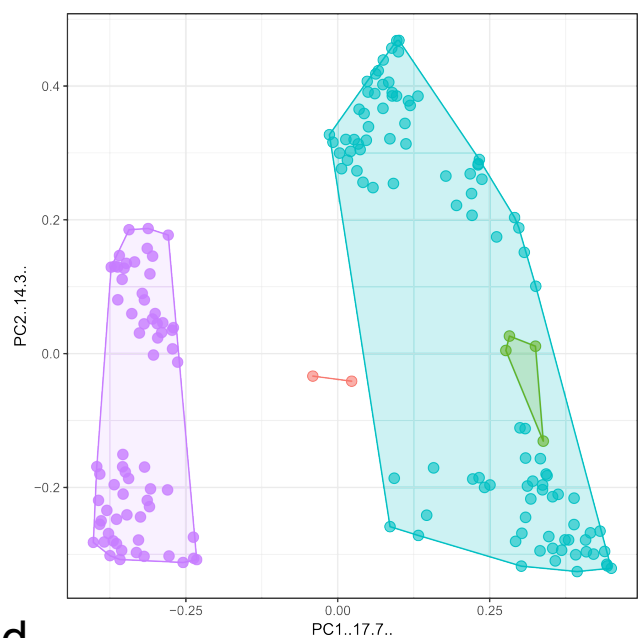
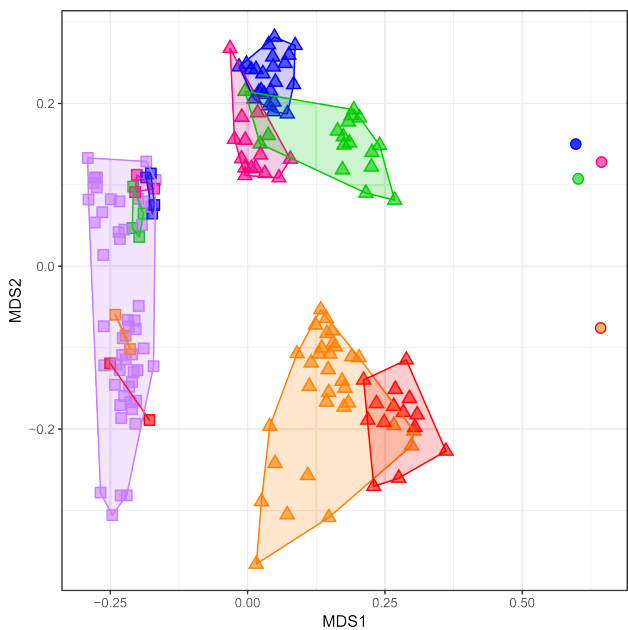
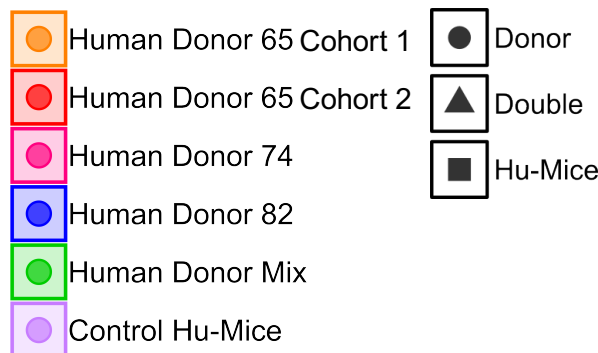
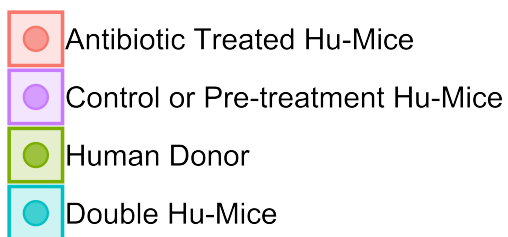
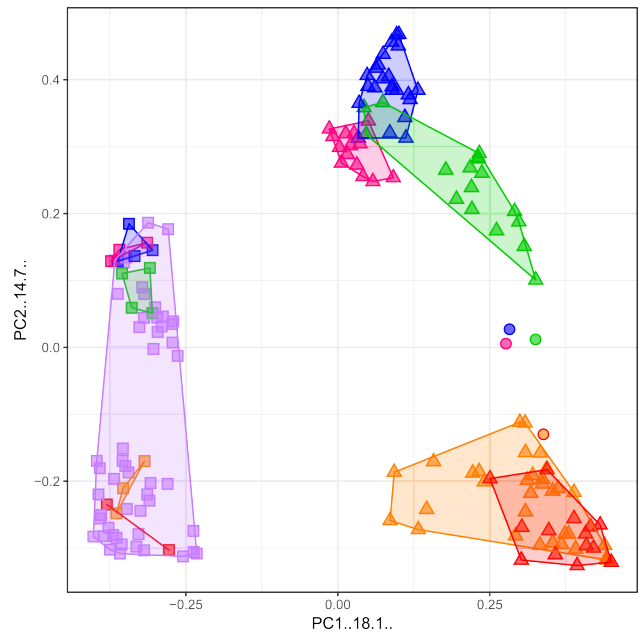
747 **Figure 7. Stability of the engrafted human-like gut microbiome in double hu-mice as**

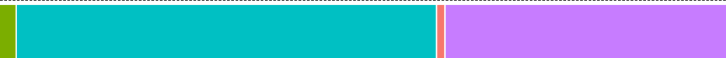
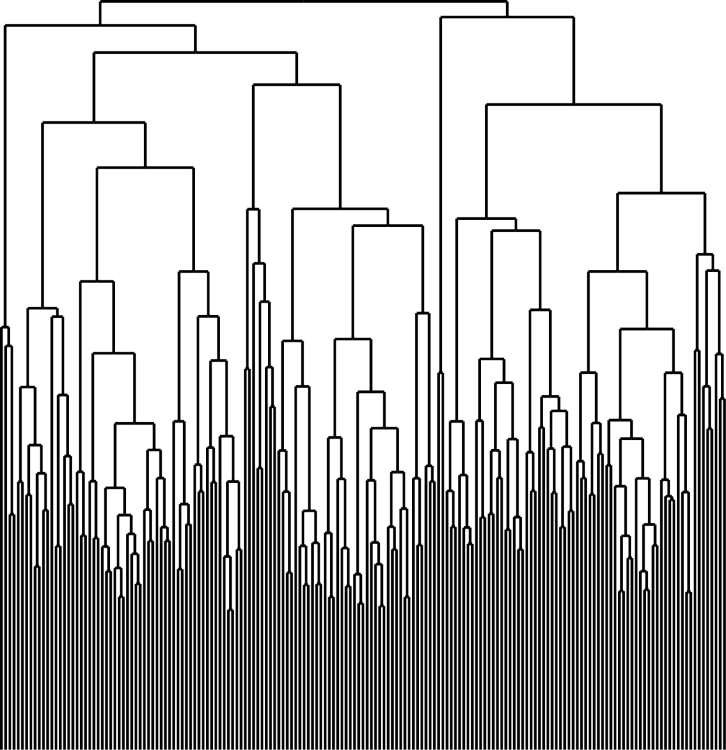
748 **determined by SourceTracker.** A) Contributions of the human fecal donor sample and pre-
749 treatment sample in the first cohort of double hu-mice created using fecal material from





750 human donor 65 (Donor 65). B) Contributions of the human fecal donor sample and pre-
751 treatment sample in the second cohort of double hu-mice created using fecal material from
752 human donor 65 (Donor 65). C) Contributions of the human fecal donor sample and pre-
753 treatment sample in double hu-mice created using fecal material from human donor 74 (Donor
754 74) or 82 (Donor 82). D) Contributions of the human fecal donor sample and pre-treatment
755 sample in double hu-mice created using a mixture of fecal material from all three human donor
756 (Donor Mix). X-axis numbers represent number of weeks post fecal transplant.

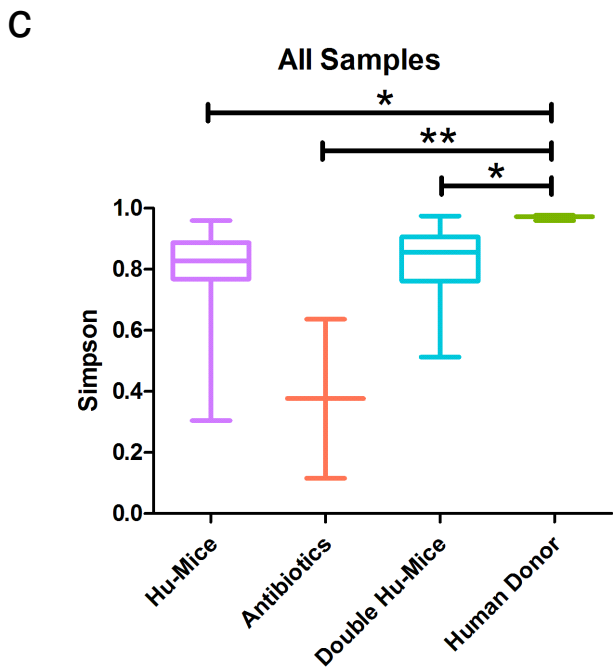
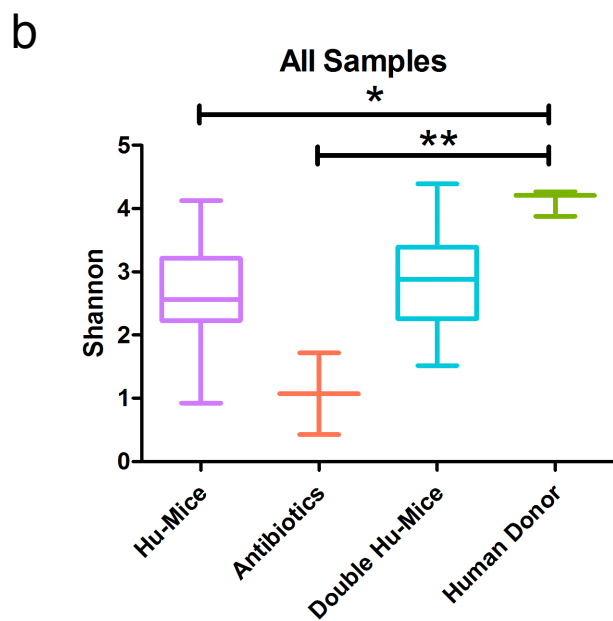
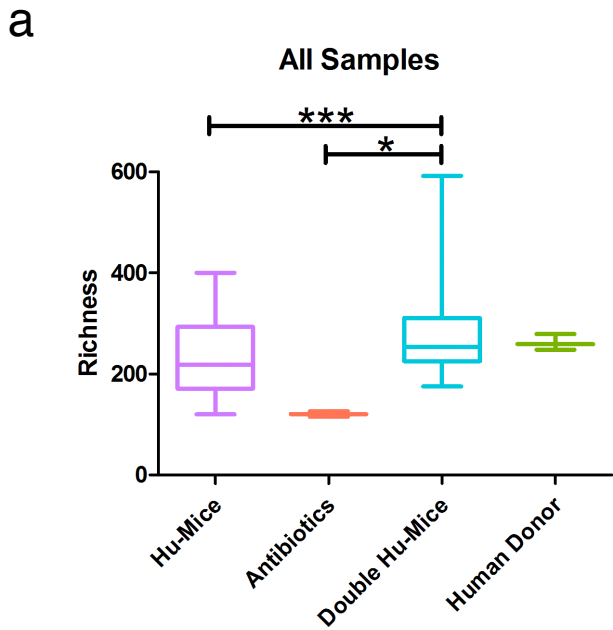
757

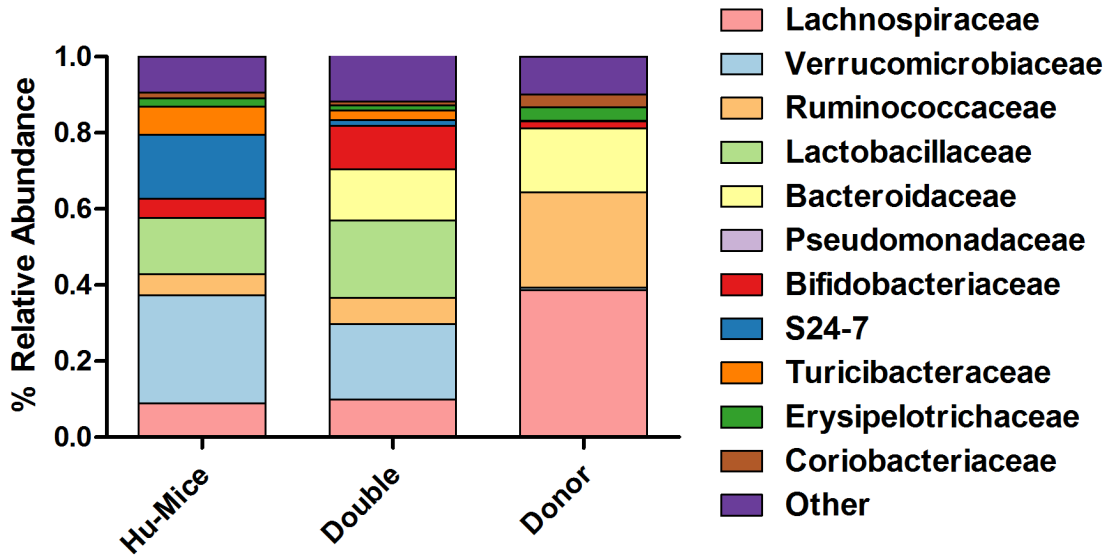
758 **Figure 8. Double hu-mice have increased human-like predicted metagenome functional**
759 **content.** A) NMDS plot displaying the double hu-mice as a distinct cluster between the human
760 fecal donor samples and pre-treatment or untreated control hu-mice. B) NMDS plot displaying
761 human donor specific functional profiles in double hu-mice. C) PCoA plot displaying the double
762 hu-mice as a distinct cluster between the human fecal donor samples and pre-treatment or
763 untreated control hu-mice. D) PCoA plot displaying human donor specific functional profiles in
764 double hu-mice.

a**b****c****d**

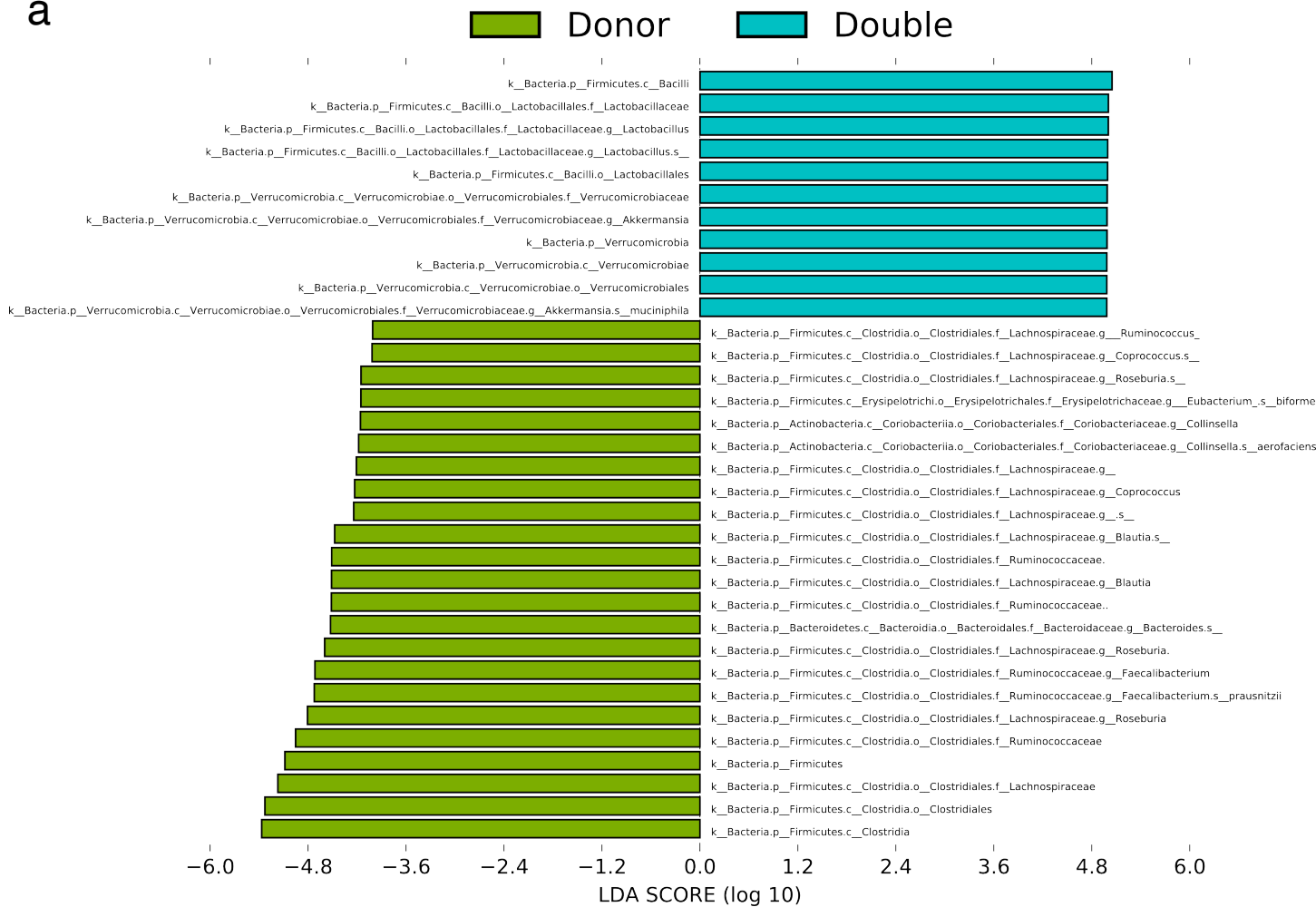


-  Human Donor
-  Double Hu-Mice
-  Antibiotic Treated Hu-Mice
-  Pre-treatment or Control Hu-Mice

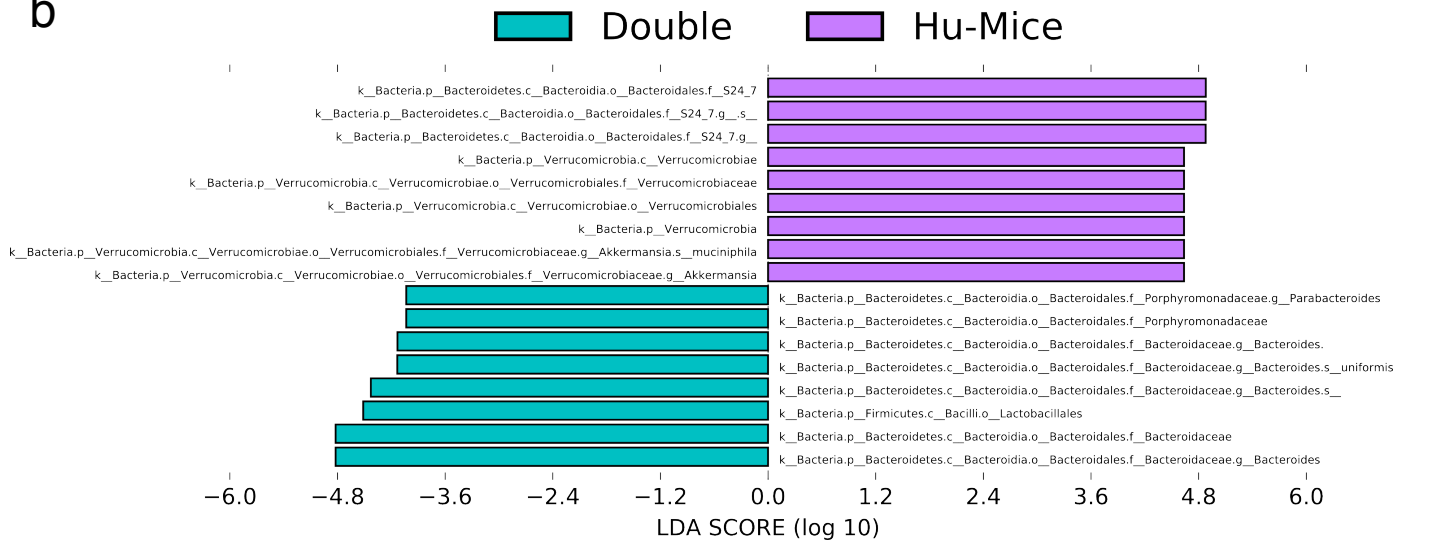


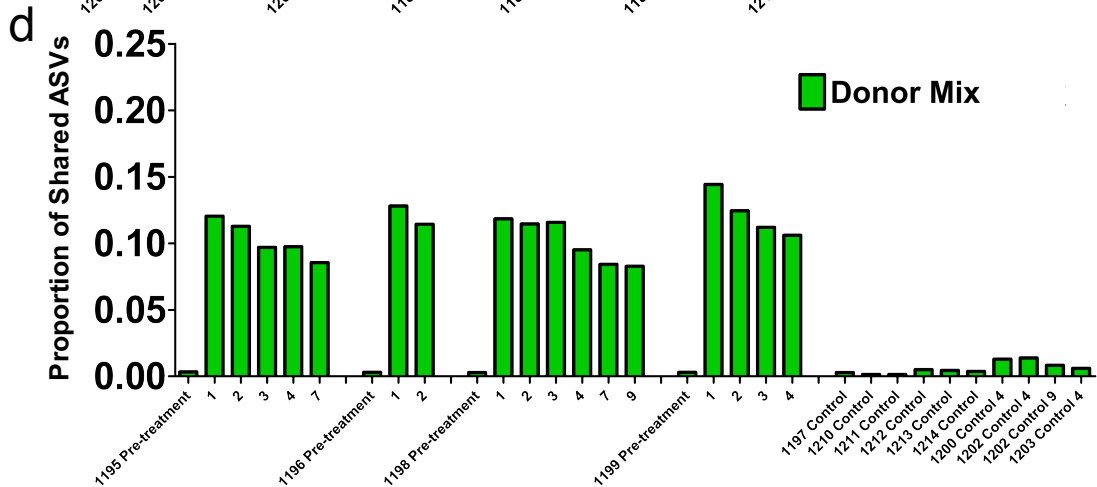
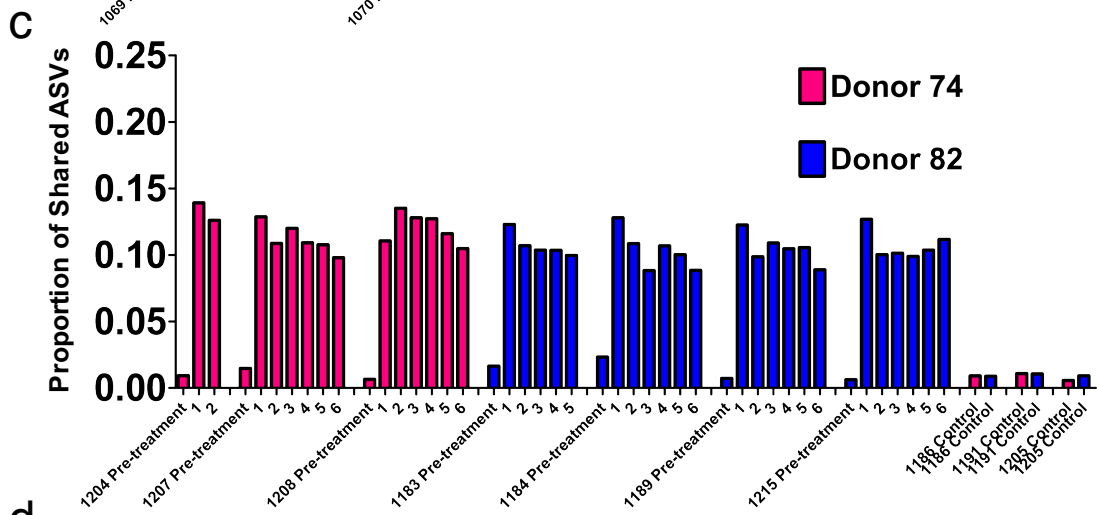
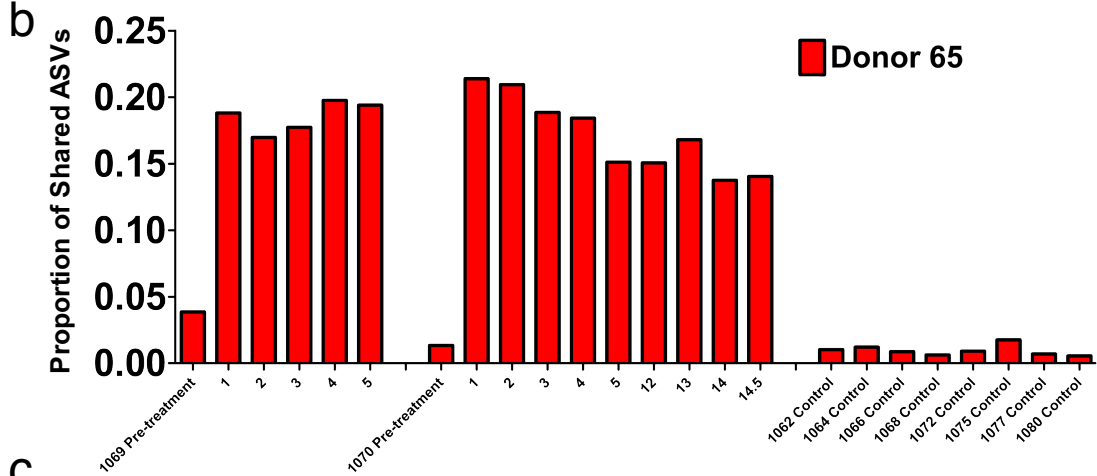
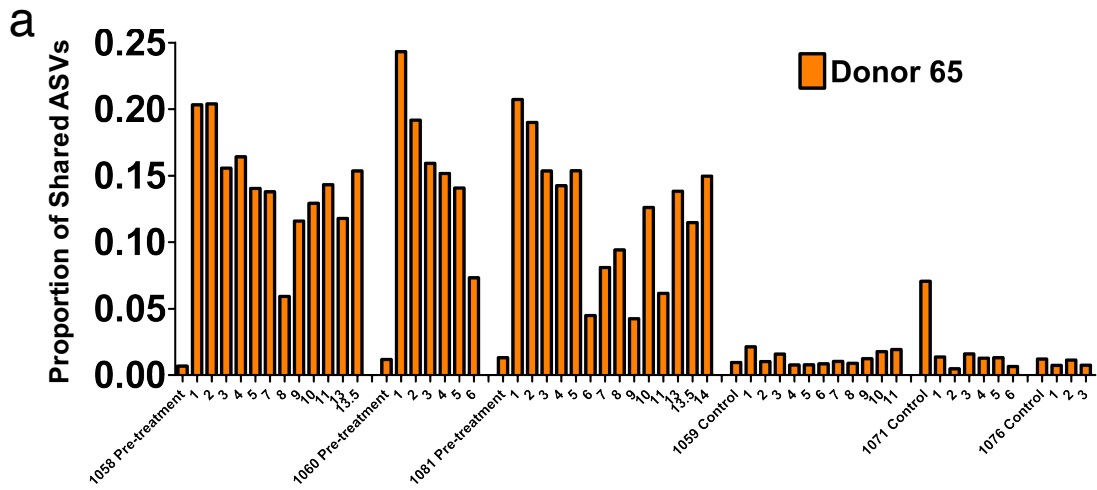


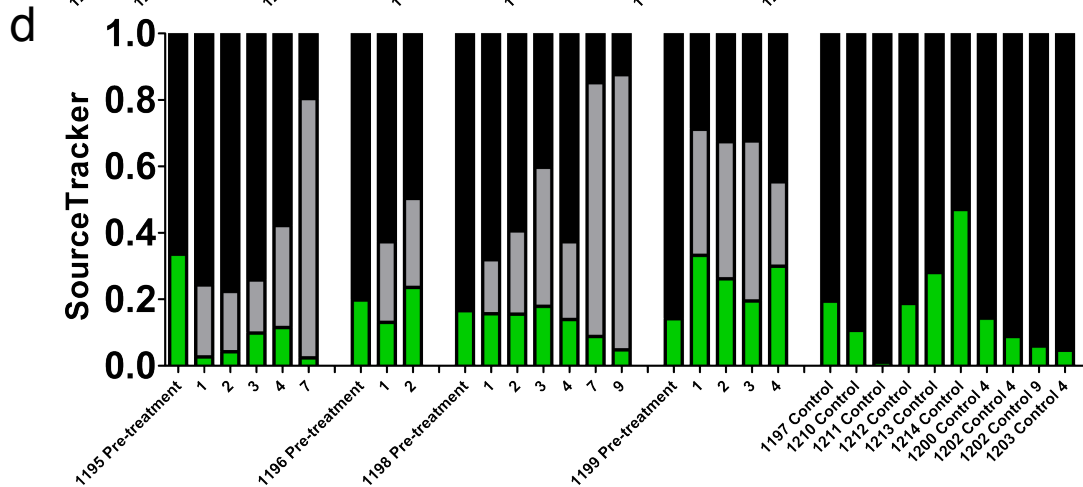
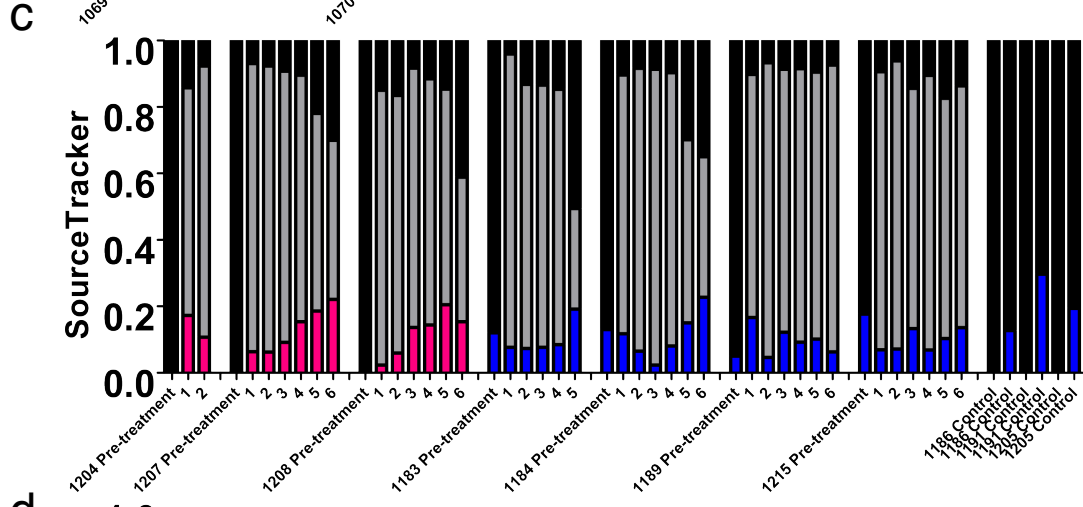
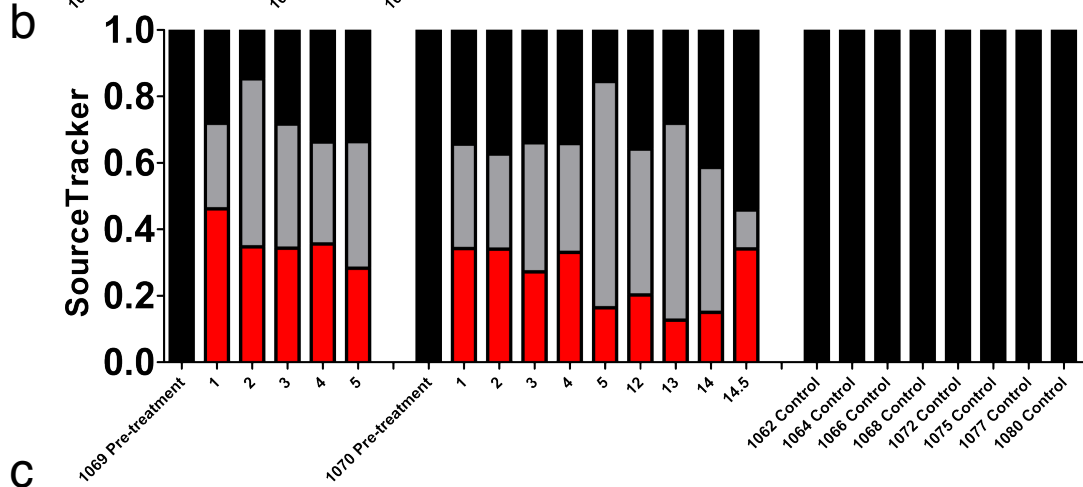
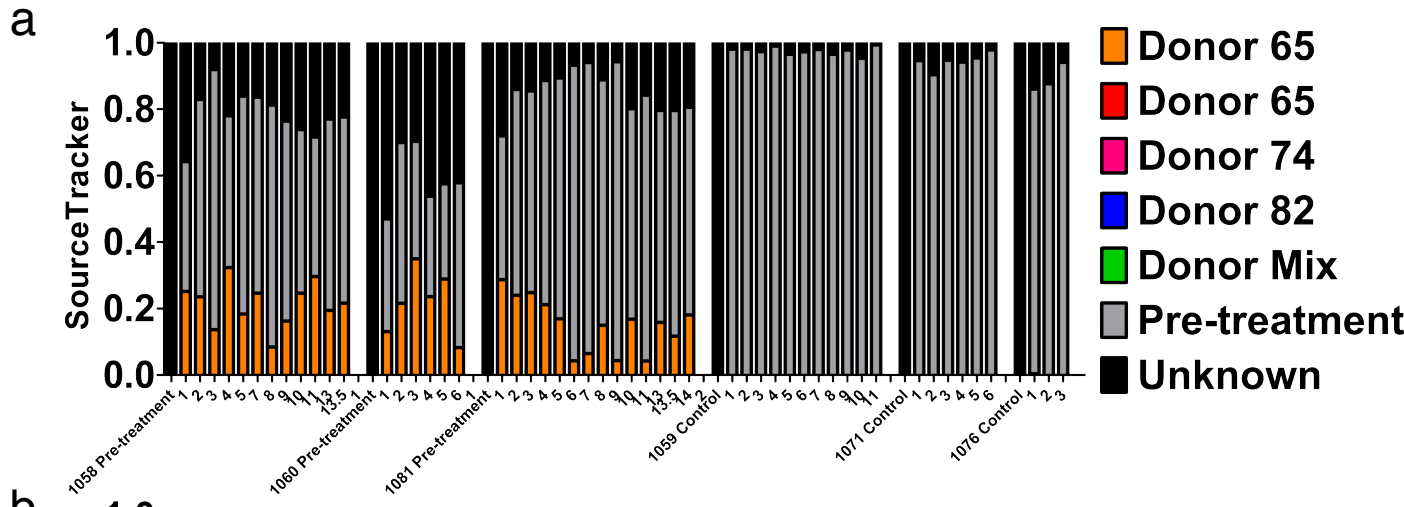
a

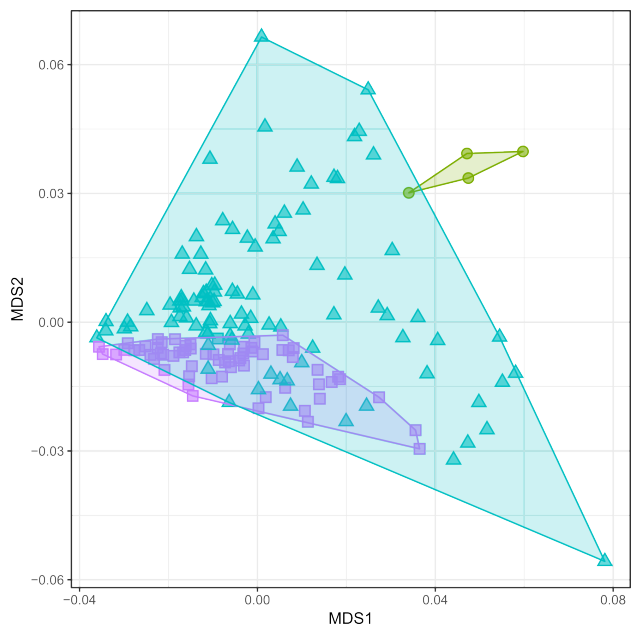
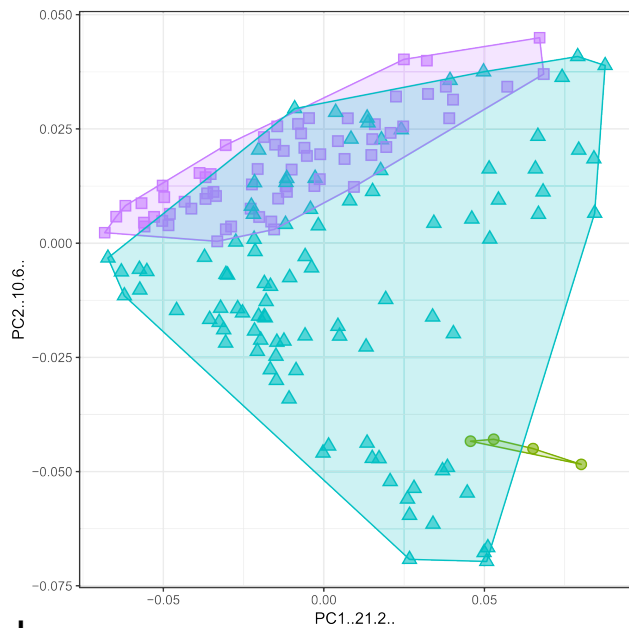
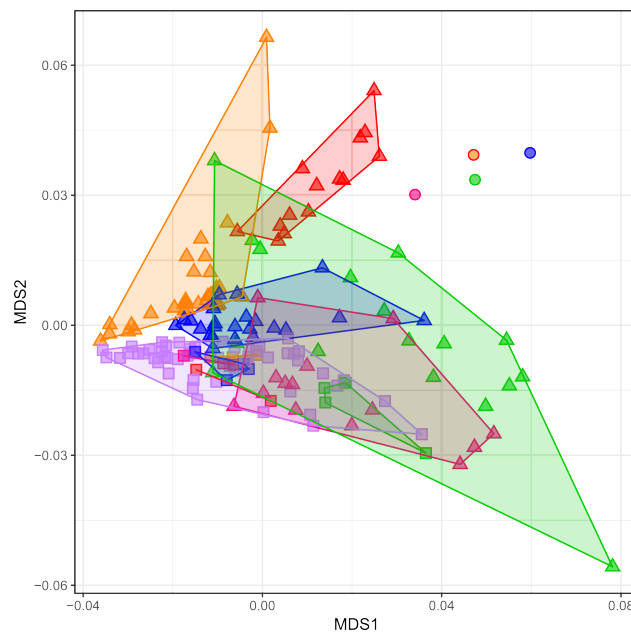


b







a**b****c****d**